Electric-field effects on magnetic anisotropy in Pd/Fe/Pd(0 0 1) surface

メタデータ	言語: eng
	出版者:
	公開日: 2017-10-03
	キーワード (Ja):
	キーワード (En):
	作成者:
	メールアドレス:
	所属:
URL	https://doi.org/10.24517/00011011

Electric-field effects on magnetic anisotropy in Pd/Fe/Pd(001) surface

Shinya Haraguchi[1], Masahito Tsujikawa[1], Junpei Gotou[1] and Tatsuki Oda[2]

[1]Graduate School of Natural Science and Technology, Kanazawa University, Kanazawa 920-1192, Japan
[2]Institute of Science and Engineering, Kanazawa University, Kanazawa 920-1192, Japan

Abstract. Electric-field (EF) effects have been studied on magnetic anisotropy in the metallic surfaces Pt/Fe/Pt(001) and Pd/Fe/Pd(001) by means of the first-principles electronic structure calculation which employs the generalized gradient approximation. The variation of anisotropy energy with respect to the EF is found to be opposite to each other. The modulus rate of the variation is larger by a few factors in the Pt substrate than in the Pd one. These results agree qualitatively well with the available experimental data. The electronic structures are presented and the origins in EF effects are discussed along a line of the second perturbative fashion.

1. Introduction

Electric-field (EF) effect of magnetic anisotropy is an important for developing a new technology of magnetic memory devices in next generations [1]. Seeking the bit-size reduction in magnetic devices, the large molar magnetic energy for retaining the memory is required so as to overcoming the thermal disturbance. Even in nano-size scale, the magnetization manipulation of such a hard magnetic material has been difficult. To overcome this problem, the EF (assisted) magnetization reversal technique is suggested. This thechnique has the advantage of low power consumption and the complicated device structure may not be so necessary for a device realization, compared with the current magnetic random access memory (MRAM) [2]. To this direction, experimental studies have been performed for magnetic semiconductors [3, 4, 5] and metallic systems [6, 7, 8]. Stimulated by such experimental works, the material search for large EF effect has been just begun in theoretical approach as well as experimental ones. It is a responsible routine to compare the trend of EF effects in similar materials. The FePd system, similar to the FePt one, is investigated in the view of EF effect on magnetic anisotropy in this work.

The systems with Fe thin layer have been used to investigate EF effects on surface magnetic anisotropy [6, 9]. In these systems, the MAE has been found to decrease as the inward EF increases, except to the case in the Fe film with Pd substrate. In the

magnetic alloy systems [7, 8, 10], the MAE also decreases as the inward EF increases. In the theoretical works [11, 12, 13] such tendency of the EF effect observed in experimental data has been obtained. The inverse EF effect in the Fe film with Pd substrate is an interesting property, which may provide a possible flexibility in designing magnetic devices. In the present work the increase of MAE is found for the Pd-substrate system, when applying an inward EF, showing a good qualitative agreement with the available experimental experience [9].

2. Method and System

We have carried out first-principles density functional calculations [14] which employ fully-relativistic ultrasoft pseudopotentials and planewave basis [15, 16]. The generalized gradient approximation (GGA) is used for the exchange-correlation energy [17]. The MAE is estimated from the total energy difference between the different magnetization directions: $\mathrm{MAE} = E_{\mathrm{tot}}^{[100]} - E_{\mathrm{tot}}^{[001]}$. In the present work we used the $30 \times 30 \times 1$ mesh in $\mathbf{k}$ point sampling [18, 19]. The equilibrium distance between Fe and Pd (Pt) atoms is not sensitive to the magnetization direction. Therefore, all the MAEs were estimated with using a fixed atomic configuration for each system. Although such distances may be changed by EF, for simplicity of the calculations and due to a metallic surface (atomic coordinates are insensitive to EF), the atomic coordinates were fixed at those of no EF.

For understanding the local contribution of MAE in real space, the MAE density, $D(\mathbf{r})$, and its integrated functions have been investigated [13]. These functions are reviewed briefly in the following. The $D(\mathbf{r})$ is estimated by ; $D(\mathbf{r}) = E_{\mathrm{tot}}^{[100]}(\mathbf{r}) - E_{\mathrm{tot}}^{[001]}(\mathbf{r})$, where the $E_{\mathrm{tot}}^{\mathbf{m}}(\mathbf{r})$ is the contribution at $\mathbf{r}$ to the total energy for the magnetization direction of $\mathbf{m}$. The $E_{\mathrm{tot}}^{\mathbf{m}}(\mathbf{r})$ may be given by

$$E_{\mathrm{tot}}^{\mathbf{m}}(\mathbf{r}) = K_{\mathbf{m}}(\mathbf{r}) + E_{\mathbf{m}}^{\mathrm{Hxc}}(\mathbf{r}) + E_{\mathbf{m}}^{\mathrm{local}}(\mathbf{r})$$
$$+ E_{\mathbf{m}}^{\mathrm{nl}}(\mathbf{r}) + U^{\mathrm{ion}}(\mathbf{r}). \tag{1}$$

$K_{\mathbf{m}}(\mathbf{r})$(kinetic energy), $E_{\mathbf{m}}^{\mathrm{Hxc}}(\mathbf{r})$(Hartreee and exchange-correlation energy) and $E_{\mathbf{m}}^{\mathrm{local}}(\mathbf{r})$(local part of pseudopotential energy) can be naturally introduced based on the original respective definitions in the ultrasoft pseudopotential method [15]. While the non-local part from the pseudopotentials has a form of $E_{\mathrm{nl}} = \sum_I E_{\mathrm{nl}}^I$ in the original scheme, in the Eq. (1) the contribution is defined by

$$E_{\mathrm{nl}} = \int_{\mathrm{cell}} E_{\mathbf{m}}^{\mathrm{nl}}(\mathbf{r}) d\mathbf{r}, \tag{2}$$

where $E_{\mathbf{m}}^{\mathrm{nl}}(\mathbf{r})$ is redefined as the linear combination of Gaussian form functions with the half width of 1.1Å centered at the atomic position. Similarly, the potential energy between the ions, $U^{\mathrm{ion}}(\mathbf{r})$, may be also defined. The MAE is alternatively obtained by $\int_{\mathrm{cell}} D(\mathbf{r}) d\mathbf{r}$. The z-dependent MAE density $\Delta(z)$ is obtained by summing $D(\mathbf{r})$ up within the in-plane unit cell in the fixed plane normal to the surface;

$$\Delta(z) = \int_{\mathrm{plane}} D(x, y, z) dx dy. \tag{3}$$

Further, we consider another integrated MAE density;

$$T(z) = \int_{-\infty}^{z} \Delta(z')dz'. \tag{4}$$

This function helps us to capture the feature of $\Delta(z)$.

In the surface system, Pd/Fe/Pd(001), there are five atomic Pd layers for the substrate (Pd(1), Pd(2), ..., from the top substrate layer), a Fe layer, and the Pd capping layer (Pd(c)). This is a slab model, as shown in Fig. 1(a). The atomic coordinates of the three bottom layers were fixed to the appropriate values of the bulk fcc Pd. The other atoms were relaxed with using the calculated atomic forces under zero EF. For Pt/Fe/Pt(001), the four Pt layers were taken for the substrate as in the previous work [13].

In order to impose the EF, which has the z-direction ([001]), we have employed the effective screening medium (ESM) method [20]. Here, some details in the present calculation are reviewed briefly. The similar applications are found in the previous reports [13, 21]. The ESM method provides the electrostatic potential (Hartree potential V_H);

$$V_H(\mathbf{r}) = \int G(\mathbf{r}, \mathbf{r}')n(\mathbf{r}')d\mathbf{r}', \tag{5}$$

where $G(\mathbf{r}, \mathbf{r}')$ and $n(\mathbf{r})$ are the Green's function and charge density, respectively. The Fourier component of G is given by

$$G(\mathbf{g}_{\parallel}, z, z') = \frac{4\pi}{2g_{\parallel}}e^{-g_{\parallel}|z-z'|} - \frac{4\pi}{2g_{\parallel}}e^{-g_{\parallel}(2z_1-z-z')}, \tag{6}$$

where the $\mathbf{g}_{\parallel}$ and $g_{\parallel}$ are the two dimensional reciprocal vector and its modulus, and the z_1 specifies the place of ESM. The first term of Eq. (6) means the kernel function of simple Coulomb interaction and the second one is introduced for effects of the mirror charge raized by the ESM of ideal conductor. In addition, the boundary conditions are imposed as follows;

$$V_H(\mathbf{g}_{\parallel}, z)\Big|_{z=z_1} = 0, \tag{7}$$

$$\frac{\partial}{\partial z}V_H(\mathbf{g}_{\parallel}, z)\Big|_{z=-\infty} = 0. \tag{8}$$

In the application, the minus infinity ($z = -\infty$) of z-coordinate is replaced by a finite practical value far from the other artifitial surface in the slab model. The ESM, as shown in Fig. 1(a), is placed away from the slab system at the distance of 0.6 nm. Some tiny number of electrons is subtracted from or added to the system for induction of the EF. The strength of EF ($\mathcal{E}$) is estimated from the slope of the electrostatic potential at the front of ESM. The Kohn-Sham equation, which contains the electrostatic potential given above, is solved in the framework of the repeated slab model.
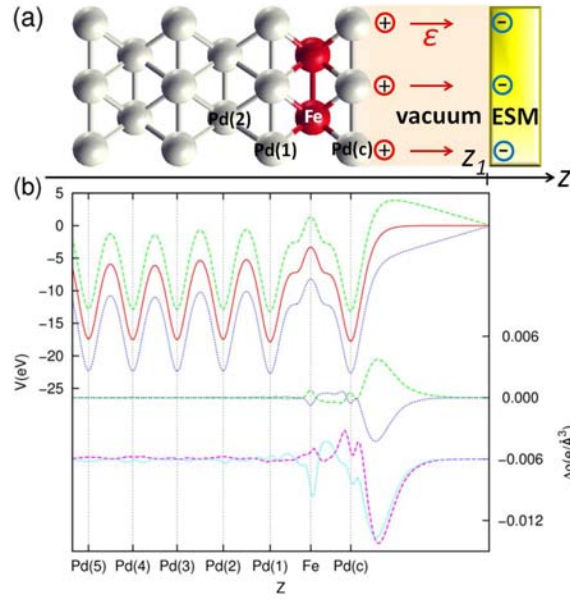
Figure 1. (color online)(a) Schematic view of the calculation model for the surface, Pd/Fe/Pd(001). (b) The upper curves present the planar-averaged electrostatic potential along z-coordinate at $\mathcal{E} = -9.6$ (green dashed curve), 0.0 (red solid curve), and 9.6 (blue dotted curve) V/nm. The lower curves present the EF-induced electron densities for majority-spin (magenta dotted curve) and minority-spin (cyan dotted curve) states at 9.6V/nm.

3. Results

3.1. Relaxed surface structures

The optimized surface structure has layer distances of 0.176, 0.179 and 0.206nm, respectively, for Pd(c)-Fe, Fe-Pd(1) and Pd(1)-Pd(2) layers. The corresponding distances in the Pt system are 0.177, 0.184 and 0.213nm, respectively. In the surface, the distance between Fe and the capping Pd (Pt) atoms is reduced by about 2% (2%) from the bond length in the regular alloy of FePd (FePt) [22].

### 3.2. Electrostatic potential and electron density

The planar-averaged electrostatic potential under the EF and EF-induced electron density are presented for the Pd system in Fig. 1 (b). The EF of $\mathcal{E} = 9.6$V/nm in the Pd system, for example, is realized under the lack of 0.04 electrons per single surface Pd atom. The potential zero is taken at the ESM. By applying the EF, the additional electron density is induced mainly at the first(Pd) and second(Fe) layers. This feature is very similar to the Pt system [13]. As well as the in the metallic systems [11, 13], the behavior of Friedel-like oscilation is observed in the EF-induced spin-separated electron densities. The period of the oscilation is different from the other spin state and at the Fe layer the changes of majority- and minority-spin states appear oppositely. The latter

may be reflected from the difference of Fermi surface between the spin states in the ferromagnetic system.

3.3. Magnetic anisotropy energy (MAE)

The MAE in the GGA calculation for Pt/Fe/Pt(001) is reduced to 7.6mJ/m^2 (zero EF: $\mathcal{E} = 0$) from the value in the local density approximation (LDA) calculation (11mJ/m^2) [13]. This is attributed to the difference of details at the Fermi level in electronic structures. Such difference between GGA and LDA is there already in Fe monolayers. The elemental data of the MAEs have been reported for magnetic transition metal monolayers [23]. Regardless of these differences, the slopes of MAE with respect to EF are found to be very similar to each other; γ(GGA)=78μJ/m^2 in 1V/nm, comparable to 72 μJ/m^2 [13].

The MAE in Pd/Fe/Pd(001) is estimated to be -0.43mJ/m^2 ($\mathcal{E} = 0$). The modulus of this value is comparable to the MAE (0.15meV/Fe, compiled to 0.30mJ/m^2) in the bulk system (multilayer system) when choosing as the same level approximation as the present work [22]. The difference of the favors (in-plane anisotropy in Pd/Fe/Pd/(001) against out-of-plane one in a Fe/Pd multilayer) may provide us a possibilty to control properties of magnetic anisotropy. EF effects on the magnetic anisotropy in Pd/Fe/Pd(001) are presented in Fig.2, compared with those of Pt/Fe/Pt(001). The MAE decreases in the Pd system and increases in the Pt one as the EF (outward EF) increases. The slope of Pd (Pt) is evaluated as $\gamma_{Pd(Pt)} = -21$ (+78) μJ/m^2 in 1V/nm. The ratio of the slopes is estimated to be $\gamma_{Pd}/\gamma_{Pt} \approx -0.27$. These signs of slopes and the ratio are in good qualitative agreement with the available experimental data [9]. The inversed slope of the Pd system may be consistent with the behaviour of MAE with respect to the number of electrons in the bulk system under a rigid band approximations [24].
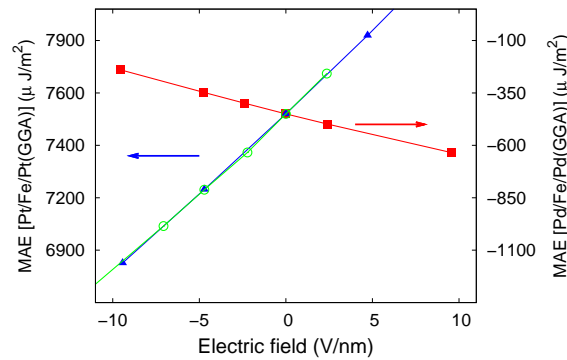
Figure 2. (color online). Magnetic anisotropy energies (MAEs) for electric fields: Pd/Fe/Pd(001)(GGA)(red squares) and Pt/Fe/Pt(001)(GGA)(blue triangles), in comparison with Pt/Fe/Pt(001)(LDA)(green circles) [13].

3.4. Magnetic anisotropy energy (MAE) density

Distribution in real space may help us to understand the behaviour of MAEs. Figure 3 shows an EF induced MAE density at 9.6V/nm for Pd/Fe/Pd(001). The local contribution of MAE changes remarkably, especially, at Pd layers. This may be understood in term of relatively large spin-orbit coupling coefficient on Pd atom. However, such local contribution almost cancels out and the MAE of whole system becomes the small value. At the Fe layer, the modulation in real space is not so large but, the local variation at Fe layer (-0.72mJ/m^2) is clearly observed in Fig. 3(b). Such feature does not indicate that the origin of MAE is lead only from Fe atom. The chemical bonding to the ligand atom and crystal field around the magnetic atom induces electronic anisotropies, resulting to the magnetic anisotropy. Note that the changes of local MAE are observed even at the deep layers where the screening effect of metallic surface should work well (see Fig. 1(b)). This indicates that the variation of MAE is not directly related to the changes of electron density.
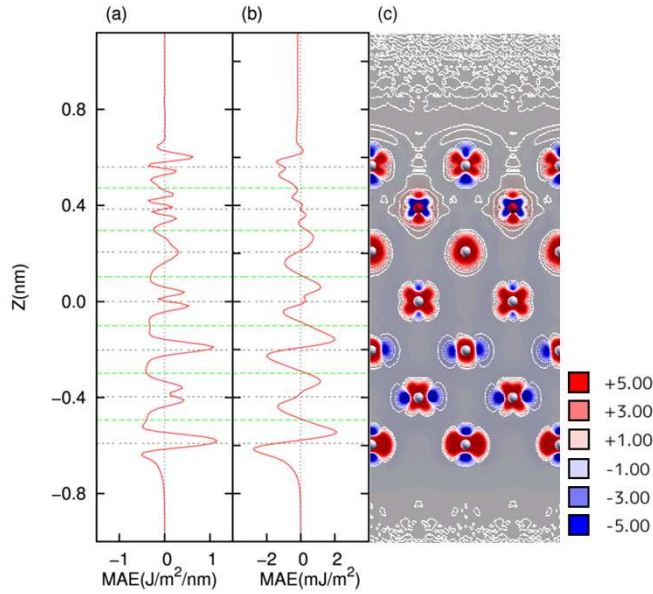
Figure 3. (color online). Electric field induced change of the magnetic anisotropy energy (MAE) densities at 9.6V/nm; (a) the planar-averaged MAE density $\Delta(z)$, (b) the function $T(z)$ obtained by integrating (a) along z-direction, (c) the MAE density map on the (110) plane which contains the Fe and Pt atoms. The horizontal thin and thick dashed lines in (a) and (b) indicate the atomic z-coordinates and the layer boundaries (intermediate of z-coordinates), respectively.

3.5. Density of states and magnetic moments

In order to analyse origins of the reversed slope of MAE in Pd/Fe/Pd(001), the basic electronic structures and the magnetic properties are presented in the following

subsections. Figure 4 shows the local density of states (LDOS) at zero EF for the d orbital on Fe atom and the capping atom (Pd(c) or Pt(c)) in Pd/Fe/Pd(001) and Pt/Fe/Pt(001). There is a large exchange splitting for Fe atoms. The spin magnetic moments are reported in Table 1. These values are consistent with the previous works [22]. In comparison with the LDA result [25], the atomic spin magnetic moment of Fe atom in Pt/Fe/Pt(001) is slightly increased at GGA, which coincides with the typical trend between LDA and GGA.

Interestingly, the exchange splitting between spin-up and spin-down states is clearly observed in the Pd and Pt bands. Indeed, the spin magnetic moment has $0.3\mu_{\mathrm{B}}$ on both Pd(c) and Pt(c). In contrary, those on atoms in the Pd substrate (Pd(1), Pd(2), ··, etc.) are larger than in the Pt one. A clear contrast is observed at the spin magnetic moment in the second substrate monolayer (see Table 1, $0.19\mu_{\mathrm{B}}$ on Pd(2) against $0.02\mu_{\mathrm{B}}$ on Pt(2)). These properties reflect to the difference in the total spin magnetization between Pd/Fe/Pd(001)($4.9\mu_{\mathrm{B}}$) and Pt/Fe/Pt(001)($3.8\mu_{\mathrm{B}}$). Such subtle prior appearance of magnetism at Pd element has been reported in the literatures for nano-systems [26].

The Fe components of LDOS in the Pt system extend to a wider range in energy than those in the Pd one. Associated with this property, the Pt components also form a wider band, compared with the Pd. These imply that in the former the hybridization of Fe d orbitals with the nonmagnetic metal d orbitals is even larger than that in the latter.

The orbital magnetic moments are also collected in Table 1. The orbital moments on Fe and Pt in Pt/Fe/Pt(001) are very similar to those obtained in LDA [25]. The difference of orbital magnetization ($0.003\mu_{\mathrm{B}}$ on Fe in Pt/Fe/Pt(001)) between the [001] and [100] magnetization directions is decreased in GGA, compared with the result of LDA [25]. If the simple Bruno's relation [22, 27] is allowed to apply separately only on Fe atom, such decrease may imply the decrease of MAE in GGA (see subsection 3.3).

In Table 1, we also show EF induced values on the spin and orbital magnetic moments. All induced values are very small at the EFs, compared with the usual experimental accuracy.

3.6. Angular components for LDOS

Figure 5 shows the LDOS for Fe $3d$ orbitals (d_{xy}, d_{xz}, $d_{3z^2-r^2}$, d_{yz}, $d_{x^2-y^2}$) in the Pd and Pt systems. The density of states is similar to the counterpart in the other system. In both systems, the minority spin states at the Fermi level are relatively small in d_{xy}, d_{xz}, d_{yz} components. In Pt/Fe/Pt(001), the large MAE is attributed to a strong hybridization of Fe $3d$ orbitals with Pt $5d$ ones [25]. This is because the low densities of d_{xz} and d_{yz} components around the Fermi level decouple the effective spin-orbit interaction between the occupied and unoccupied states, reducing a favor of in-plane magnetic anisotropy (see the first paragraph in section 4).

In Pd/Fe/Pd(001), the corresponding angular components (d_{xz} and d_{yz}) have been kept to an amount of density with a definitive peak above the Fermi level (at 0.5
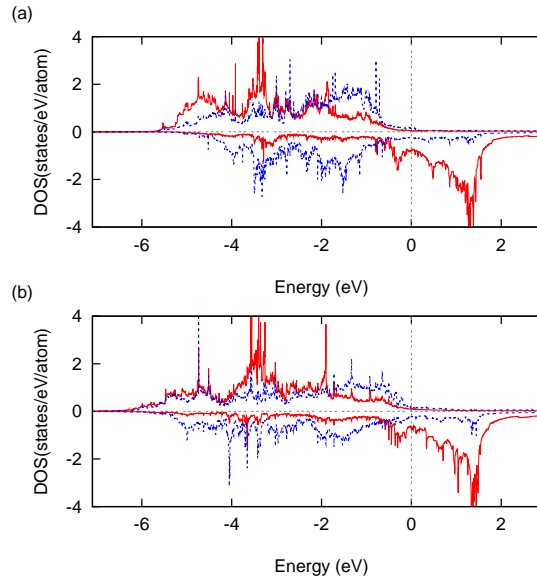
Figure 4. (color online). The local density of states for (a) Pd/Fe/Pd(001) and (b) Pt/Fe/Pt(001). The red full and blue dashed curves indicate the d-component of Fe and that of the capping metal (Pd or Pt), respectively.

eV). This may be due to a weaker hybridization with the Pd $4d$. The couplings with $d_{3z^2-r^2}$, d_{xy}, and $d_{x^2-y^2}$ through spin-orbit interaction always favors a reduction of MAE, resulting in the small value of MAE for the Pd system. The electronic structure in momentum space is also important and described in the next subsection.

3.7. Band dispersion curves

Figure 6 shows band dispersion curves in Pd/Fe/Pd(001). The predominant Fe $3d$ components are indicated by symbols when the ratio of component is larger than 0.1. These indications present a partial preservation of properties in the Fe monolayer [24, 28]. There are many regions modified by the hybridization with the non-magnetic metal atoms; $d_{3z^2-r^2}$ components at $\bar{\text{X}}$ below the Fermi level, $d_{xz,yz}$ at $\bar{\text{X}}-\bar{\Gamma}$ line smears out below the Fermi level again, and $d_{x^2-y^2}$ around $\bar{\text{X}}$ becomes below the Fermi level, and so on. The distribution of symbols for angular components is very similar to that of Pt/Fe/Pt(001) [25]. This implies that there is a similarity in the electronic structure of Pt/Fe/Pt(001). However, in order to seek the reason of EF effects on MAE, differences in electronic structure are important. The components of d_{xy} are placed at a lower energy around $\bar{M}$, compared with the counterpart in the Pt system [25].

The location of the Fermi level may essentially be determined by the relative atomic energy level of Fe to Pd and the hybridization between their d-orbitals. The atomic $4d$ level of Pd may lower the Fermi level, compared with the system of Pt. Furthermore, as described before, Figure 4 inspires us to understand a weakness of d-orbital hybridization

Table 1. The spin and orbital magnetic moments (μ_B) at zero electric field and their electric-field-induced variations in $M/\mathrm{Fe}/M(001)(M =\mathrm{Pd}$ and Pt) for magnetization directions ([001] and [100]).

| M(V/nm)		spin				
		total	Fe	M(c)	M(1)	M(2)
Pd(0)	[001]	4.917	3.266	0.326	0.344	0.189
	[100]	4.920	3.266	0.328	0.344	0.189
Pd(9.6)	[001]	0.010	0.002	0.008	−0.001	0.001
	[100]	0.012	0.002	0.008	−0.001	0.001
Pt(0)	[001]	3.807	3.234	0.336	0.269	0.024
	[100]	3.777	3.239	0.341	0.270	0.015
Pt(4.7)	[001]	−0.003	0.000	0.004	−0.001	−0.001
	[100]	−0.003	0.001	0.004	−0.002	−0.001
		orbital				
			Fe	M(c)	M(1)	M(2)
Pd(0)	[001]		0.050	0.027	0.029	0.021
	[100]		0.045	0.040	0.034	0.020
Pd(9.6)	[001]		−0.001	0.000	0.000	0.000
	[100]		0.001	0.002	0.000	0.000
Pt(0)	[001]		0.037	0.056	0.038	0.003
	[100]		0.034	0.098	0.048	0.005
Pt(4.7)	[001]		−0.001	0.000	0.000	0.000
	[100]		0.001	0.001	−0.001	0.000

in the Pd system. Based on these properties and replacing Pt with Pd, the Fermi level may be lifted up to a higher energy with respect to the location of Fe 3d minority spin-state orbitals.

4. Discussions

Assuming a large exchange splitting like Fe atom, the MAE may be well understood by the second perturbative formula [29];

$$\mathrm{MAE} = (\xi)^2 \sum_{o,u} \frac{|\langle o|\ell_z|u\rangle|^2 - |\langle o|\ell_x|u\rangle|^2}{\epsilon_u - \epsilon_o}, \tag{9}$$

where o and u specify occupied and unoccupied minority spin states and the ℓ_x and ℓ_z are angular momentum operators. The parameter of ξ is an average of SOC coefficient. The pair of occupied and unoccupied states around the Fermi level is important. The above perturbative formula may be used for discussions on magnetic anisotropy related with Fe atom and on ligand-atom effect associated with it. Magnetic anisotropy though the hybridization with the d-orbitals of non-magnetic atom (Pd and Pt) may be influenced by its large spin-orbit coupling. This is because the ξ_Fe (0.063eV), which
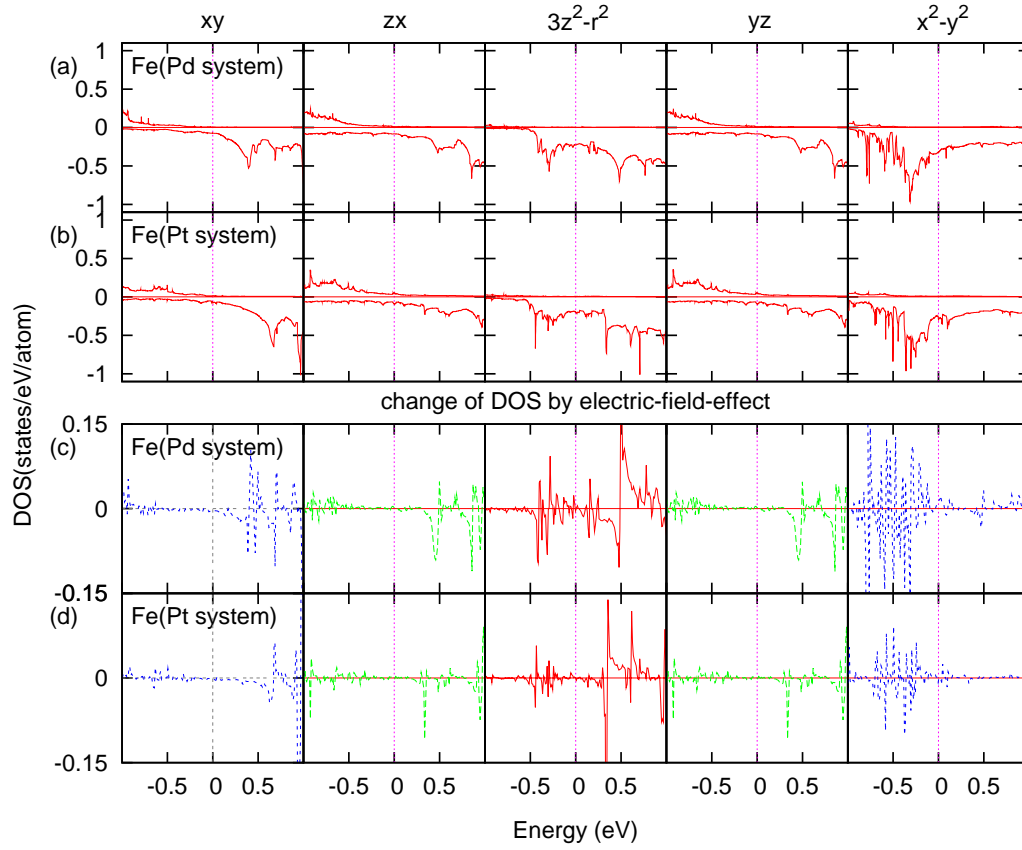
Figure 5. (color online). The local density of states for Fe 3d components in (a) Pd/Fe/Pd(001) and (b) Pt/Fe/Pt(001) at zero electric field and the electric-field induced change in (c) Pd/Fe/Pd(001) at 9.6V/nm and (d) Pt/Fe/Pt(001) at 4.7V/nm. The vertical lines indicate the Fermi level.

can be estimated in the atomic calculation, is much smaller than those of Pd and Pt (ξ_{Pd} =0.22eV and ξ_{Pt} =0.54eV). The magnetic anisotropy which solely comes from the Pd and Pt atoms is out of consideration in Eq.(9).

Figure 7 shows the comparison of the band dispersion curves between the zero EF and 9.6V/nm in Pd/Fe/Pd(001). In this figure, the Fermi levels are fixed to zero energy and the each symbol is placed when the ratio of the component is larger than 0.1. Due to the decrease of number of electrons at 9.6V/nm, the predominant sysmbols which indicate the Fe 3d minority-spin component are raised up to a higher enegy at many places in reciprocal space. These changes are similar to the rigid band shift and most of them are subtle ones. However, some of remarkable ones are observed on the $\bar{X} - \bar{\Gamma}$ line around 0.45eV in $d_{3z^2-r^2}$ and $d_{yz(xz)}$ components and aroud $\bar{M}$ at 0.4eV in d_{xy} component. Such EF-induced change, appearing as remarkable ones in LDOS (described below), is important to understand the orgin of EF variations on MAE.

Figure 5 shows the EF induced change in LDOS for both systems; 9.6V/nm and 4.7V/nm in the Pd and Pt systems, respectively. The changes in the Pt are consistent with the increasing behaviour of MAE; the behaviours about the pair of peaks just below
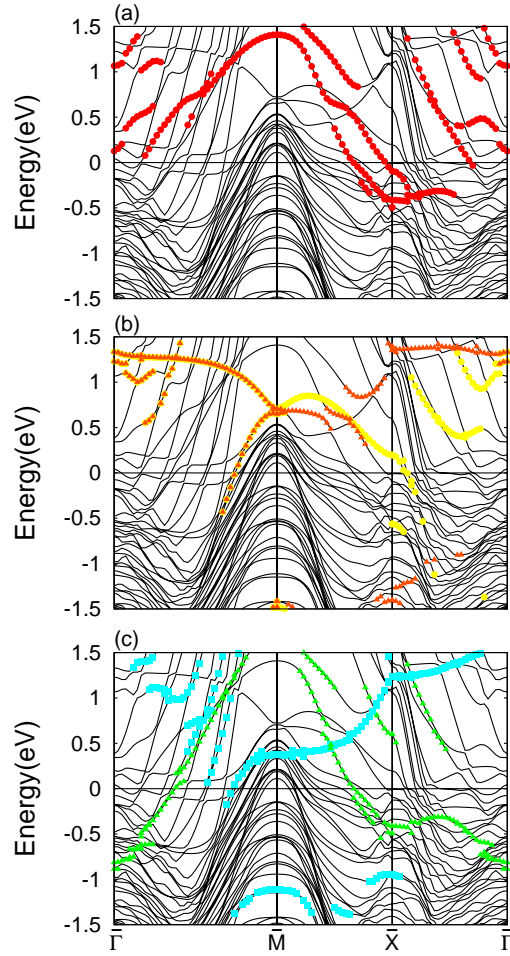
Figure 6. (color online). Band dispersion curves in Pd/Fe/Pd(001) for zero electric field. The predominant components of Fe 3d orbitals ($d_{3z^2-r^2}$, d_{xz}, d_{yz}, d_{xy} and $d_{x^2-y^2}$) for minority-spin states are marked as, respectively, (a) red circles, (b) orange triangles, yellow circles, (c) blue squares, and green triangles. The horizontal lines indicate the Fermi level.

and above the Fermi level in $d_{3z^2-r^2}$ (large DOS at the Fermi level) and $d_{xz(yz)}$ (decrease at 0.3eV) favor the out-of-plane anisotropy (see Eq.(9) and the behaviour about the pair in $d_{x^2-y^2}$ and $d_{xz(yz)}$ also out-of-plane. For the Pd system, there is a minus peak (dip) above the Fermi level at d_{xy} (at 0.3eV) in Fig. 5. The coupling with $d_{x^2-y^2}$ may favor a reduction of out-of-plane anisotropy and the coupling between the minus peak at $d_{xz(yz)}$ in Fig. 5 and $d_{3z^2-r^2}$ (large DOS) favor a reduction of in-plane anisotropy. Therefore, there may be some cancellations and the inverse of EF effect in the Pd system may appear as a result of the subtle imbalance of electronic structure modulations.

Origins of the reversed slope in EF dependence in the Pd system have not been definitively identified in this work. In general description, the MAE is a physical quantity
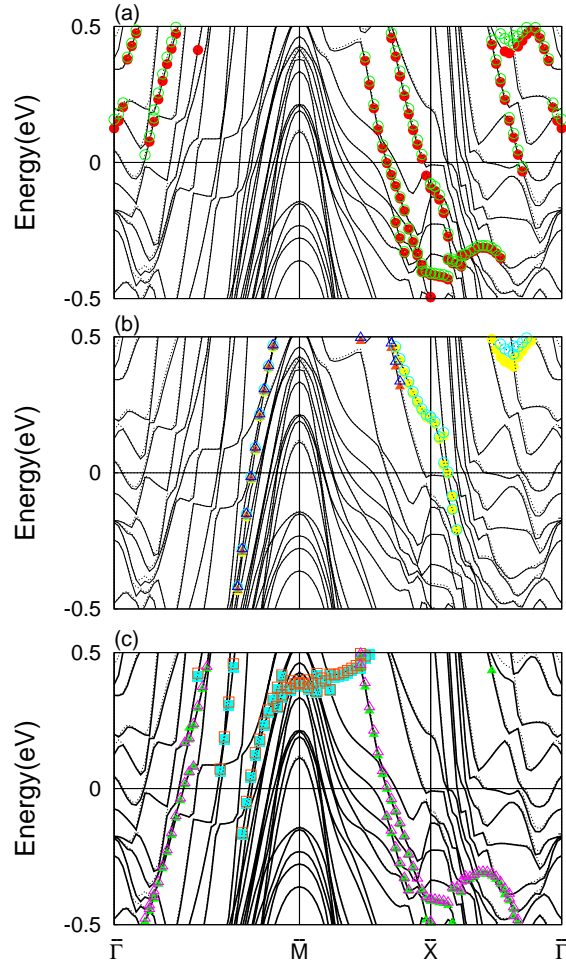
Figure 7. (color online). Band dispersion curves in Pd/Fe/Pd(001) for zero electric field (solid curves) and 9.6V/nm (dotted curves). In the zero electric field (9.6V/nm), the predominant components of Fe $3d$ orbitals ($d_{3z^2-r^2}$, d_{xz}, d_{yz}, d_{xy} and $d_{x^2-y^2}$) for minority-spin states are marked as, respectively, (a) red filled (green empty) circles, (b) orange filled (blue empty) triangles, yellow filled (cyan empty) circles, (c) blue filled (orange empty) squares, and green filled (magenta empty) triangles. The horizontal lines indicate the Fermi level.

very sensitive to details of the Fermi level. As presented in the previous section (section 3), there are subtle differences in the electronics structure around the Fermi level (The most rational difference may be the electronic structure of Fe d_{xy} component around $\bar{M}$) . These may be related with properties of the slightly weak orbital hybridization of Fe $3d$ with Pd $4d$ and the enhanced spin-polarization at Pd atoms. In the preliminary calculation for a pure Pd thin layer (system with five mono-atomic layers), a weak inversed EF effect is observed.

The total MAE is estimated from the couple of contributions; the electronic band

structure contribution (E_b), which is investigated in this work, and the magnetostatic contribution (E_s). Such magnetostatic interaction contributes to an in-plane anisotropy ($E_s \sim -0.39\text{mJ/m}^2$ [30]). This promotes the band contribution ($E_b = -0.43\text{mJ/m}^2$ in Pd/Fe/Pd(001) as described in subsection 3.3), being in an in-plane anisotropy at zero EF. From our calculated result of the MAE slope with respect to EF, the anisotropy of the Pd system can become an out-of-plane magnetic one when applying inward (minus) EFs ($\sim -39\text{V/nm}$). The present result of in-plane magnetic anisotropy may be consistent with the recent observation of x-ray magnetic circular dichroism (XMCD) measurement for the fine-controlled wedge-shape surface system of Pd/Fe/Pd(001) [31]. Contrarily, the out-of-plane anisotropy was persistent in the observation in which the system has a few nm thick of FePd layer [9].

5. Summary

We have investigated the MAE and its EF effects in the Pd/Fe/Pd(001) surface, in comparison with those in Pt/Fe/Pt(001). The Pd system was found to have a contribution of in-plane magnetic anisotropy from the electronic structures in the present work. Compared with the system of Pt/Fe/Pt(001), the change rate of MAE with respect to the EF showed the good qualitative agreement with the experimental data, confirming a theoretical evidence for the measured EF effects in the Pd system. The fact that the Fe layer with Pd can provide a reversed behaviour with respect to EF could provide a wide possibility to design an EF control of ferromagnet.

References

[1] Bader S D, Parkin S S P, 2010 *Annu. Rev. condens. Matter Phys.* **1** 71
[2] Slonczewski J C 1996 *J. Magn. Magn. Mater.* **159** L1
[3] Ohno H, Chiba D, Matsukura F, Omiya T, Abe E, Deitl T, Ohno Y and Ohtani K 2000 *Nature* **408** 944
[4] Chiba D, Yamanouchi M, Matsukura F and Ohno H 2003 *Science* **301** 943
[5] Chiba D, Sawicki M, Nishitani Y, Nakatani Y, Matsukura F and Ohno H 2008 *Nature* **455** 515

[6] Maruyama T, Shiota Y, Nozaki T, Ohta K, Toda N, Mizuguchi M, Tulapurkar A A, Shinjo T, Shiraishi M, Mizukami S, Ando Y, Suzuki Y 2009 *Nature Nanotech.* **4** 158

[7] Shiota Y, Maruyama T, Nozaki T, Shinjo T, Shiraishi M and Suzuki Y 2009 *Appl. Phys. Express* **2** 063001

[8] Nozaki T, Shiota Y, Shinjo T and Suzuki Y 2010 *Appl. Phys. Lett.* **96**, 022506.

[9] Weisheit M, Fähler S, Marty A, Souche Y, Poinsignon C and Givord D 2007 *Science* **315** 349

[10] Endo M, Kanai S, Ikeda S, Matsukura F and Ohno H 2010 *Appl. Phys. Lett.* **96** 212503.

[11] Duan C G, Velev J P, Sabirianov R F, Zhu Z, Chu J, Jaswal S S and Tsymbal E Y 2008 *Phys. Rev. Lett.* **101** 137201

[12] Nakamura K, Shimabukuro R, Fujiwara Y, Akiyama T, Ito T and Freeman A J 2009 *Phys. Rev. Lett.* **102** 187201

[13] Tsujikawa M and Oda T 2009 *Phys. Rev. Lett.* **102** 247203

[14] Oda T, Pasquarello A and Car R 1998 *Phys. Rev. Lett.* **80** 3622

[15] Laasonen K, Pasquarello A, Car R, Lee C and Vanderbilt D 1993 *Phys. Rev. B* **47** 10142

[16] Oda T and Hosokawa A 2005 *Phys. Rev.* B **72** 224428

[17] Perdew J P, Chevary J A, Vosko S H, Jackson K A, Pederson M R, Singh D J and Fiolhais C 1992 *Phys. Rev. B* **46** 6671

[18] Monkhost H J and Pack J D 1976 *Phys. Rev. B* **13** 5188

[19] For testing a dense **k** point mesh of 48×48×1, the MAE at $\mathcal{E} = 0$ and the slope are increased by 24 and 12 %, respectively.

[20] Otani M and Sugino O 2006 *Phys. Rev. B* **73** 115407

[21] Tsujikawa M and Oda T 2009 *J. Phys.: Condense. Matter* **21** 064213

[22] Ravindran P, Kjekshus A, Fjellvåg H, James P, Nordström L, Johansson B and Eriksson O 2001 *Phys. Rev. B* **63**, 144409

[23] Wu R, Freeman A J 1999 *Journal of Magn. Magn. Mater.* **200** 498

[24] Daalderop G H O, Kelly P J and Shuurmans M F H 1991 *Phys. Rev. B* **44** 12054

[25] Tsujikawa M, Hosokawa A and Oda T 2008 *Phys. Rev. B* **77** 054413

[26] Shinohara T, Sato T and Taniyama T 2003 *Phys. Rev. Lett.* **91** 197201

[27] Bruno P 1989 *Phys. Rev. B* **39** 865

[28] Nakamura K, Ito T and Freeman A J 2003 *Phys. Rev.* B **67** 014420

[29] Wang D S, Wu R and Freeman A J 1993 *Phys. Rev. B* **47** 14932

[30] Szunyogh L, Újfalussy B and Weinberger P 1995 *Phys. Rev.* B **51** 9552

[31] Ueno T, Nagira M, Tohoda S, Tagashira T, Kimura A, Sawada M, Namatame H and Tanighchi M 2008 *e-J. Surf. Sci. Nanotech.* **6** 246